

Pulse dynamics in actively mode-locked lasers with frequency shifting

S. Longhi

INFN, Dipartimento di Fisica, Politecnico di Milano, Piazza Leonardo da Vinci, 32, I-20133 Milano, Italy

(Received 15 July 2002; published 21 November 2002)

The dynamics of wave packet splitting in a dissipative Schrödinger-like dynamical system is theoretically studied by considering the model of an amplitude-modulated mode-locked laser with frequency shifting provided by an intracavity frequency modulation. It is shown that as the strength of the frequency modulation is increased, a bifurcation takes place which corresponds to a transition from a single-pulse steady-state oscillation to a two-pulse coherent oscillatory dynamics. An analytical model for pulse splitting bifurcation and onset of two-mode oscillatory dynamics, based on a Gaussian pulse analysis, is presented and compared with numerical simulations.

DOI: 10.1103/PhysRevE.66.056607

PACS number(s): 42.79.-e, 82.40.Bj, 42.60.Fc, 42.60.Mi

I. INTRODUCTION

The method of active mode locking of lasers is a powerful means for the generation of ultrashort laser pulses, which has been extensively studied both theoretically and experimentally since a long time (for earlier references on this subject see, e.g., Refs. [1–4], and references therein). Though major efforts on active mode locking have been devoted to the achievement of clean and stable short laser pulses to be used in applications, it has been recently recognized that this operational regime hides several involved and interesting dynamical phenomena that provide a remarkable realization in the optical context of rather universal dynamical features found in dissipative dynamical systems [5–7]. In the simplest case of an amplitude-modulated (AM) mode-locked laser with an exact synchronism between the modulation period of cavity losses and the cavity round-trip time, the pulse dynamics inside the laser cavity is described by the Schrödinger equation of the quantum harmonic oscillator [3], but with the complex time transformation $t \rightarrow it$, which makes the dynamics nonconservative. As compared to the wave packet dynamics of corresponding conservative harmonic oscillator, which can show coherent oscillations due to interference of initially excited higher-order modes, the complex time transformation makes the dynamics quite trivial in the dissipative case since the fundamental Gaussian mode is always the only one that survives after transient, the higher-order Hermite-Gaussian modes being damped out. Despite this, the inclusion of perturbations, albeit small, in the pulse dynamics may strongly destroy this simple scenario. In particular, it is well known that a pulse-train instability in AM mode-locked lasers is commonly observed when the modulation frequency is detuned, even slightly, from the cavity free spectral range (see, e.g., Refs. [8–10], and references therein); detailed numerical simulations [5,11,12] have confirmed the onset of the instability and revealed its sensitivity to the noise level present in the system. Such an instability, which is analogous to the drift instability encountered in other optical and hydrodynamic systems [5], has recently found [6] a rather elegant explanation in terms of the strong non-normal transient growth of weak perturbations induced by time detuning, a generic feature of non-normal dissipative

dynamical systems which has been proposed as a general mechanism for turbulence in hydrodynamics [13]. Analogously, in case of frequency-modulated (FM) lasers it has been recognized [7] that the transition region between frequency modulation laser oscillation and FM mode locking [14,15] shows large excess noise levels, a scenario usually encountered in non-Hermitian dissipative systems (see, e.g., Refs. [16,17]). Finally, the existence of transient coherent oscillations in the spectrum of a weakly dissipative FM-operated laser, analogous to Bloch oscillations found in other optical systems [18], have been recently predicted and observed in a solid-state laser [19].

In this paper we investigate the pulse dynamics in amplitude-modulated mode-locked lasers in presence of frequency shifting induced by an intracavity frequency modulation and reveal the existence of a pulse splitting bifurcation. The frequency-shift-induced bifurcation corresponds to a coherent two-pulse oscillatory dynamics which resembles the coherent two-mode dynamics found in many conservative dynamical systems, such as in quantum dynamical tunneling [20] or in coupled waveguides [21]. The pulse splitting bifurcation provided by our model is nevertheless of purely dissipative nature and is therefore rather distinct from different mechanisms of wave packet splitting previously predicted in other conservative physical systems, such as the dynamic splitting (dichotomy) of wave packets exhibited by an electron bound by an atomic potential subjected to a strong laser field [22] or the wave packet splitting of a Bose-Einstein condensate in a periodically shaken trap [23].

The paper is organized as follows. In Sec. II the model of an AM actively mode-locked laser with frequency sliding produced by an intracavity phase modulation is introduced and the eigenmode analysis, revealing the existence of a pulse splitting bifurcation, is presented. In Sec. III a Gaussian pulse analysis of the mode-locking master equation is presented and an analytical model for the pulse splitting transition is derived. In Sec. IV the pulse dynamics in the parameter region corresponding to pulse splitting, which takes into account for the gain dynamics, is investigated by means of an eigenmode expansion analysis and by a direct numerical analysis of the mode-locking master equation. Finally, in Sec. V the main conclusions are outlined.

II. BASIC MODEL AND MODE-LOCKING ANALYSIS

A. Mode-locking master equation

We consider a homogeneously broadened laser with a slow gain medium containing an amplitude modulator, that introduces a sinusoidal change of cavity loss rate at a frequency ω_m close to the cavity axial mode separation $\Delta\omega_{ax}$, and a phase modulator that varies sinusoidally the optical cavity length at a harmonic frequency $m\omega_m$, where m is an integer. The phase modulator is used to introduce a continuous frequency shift of the intracavity pulse; to this aim, the FM signal is assumed to be shifted with respect to the AM signal such that in correspondence of the minima of loss modulation the FM signal is nearly linear, producing a frequency drift of the pulse at each transit. The evolution equation for the pulse envelope $\psi(t, T)$ at successive transits in the cavity reads (see e.g., Refs. [3,6,12,19])

$$\begin{aligned} \frac{\partial\psi}{\partial T} &= (g-l)\psi + \left\{ -\gamma\frac{\partial}{\partial t} + \mathcal{D}_g\frac{\partial^2}{\partial t^2} + \Delta[\cos(2\pi t) - 1] \right. \\ &\quad \left. - i\Delta_f\sin(2\pi mt) \right\} \psi \\ &\equiv (g-l)\psi + \mathcal{L}(t)\psi. \end{aligned} \quad (1a)$$

In Eq. (1a), t is the fast time variable, normalized to the AM period $T_m = 2\pi/\omega_m$, describing the intracavity pulse envelope shape ($-1/2 < t < 1/2$); T is the round-trip number, which accounts for the slow change of the pulse envelope at successive transits in the cavity; $\gamma \equiv (\Delta\omega_{ax} - \omega_m)/\omega_m$ is the frequency detuning parameter ($|\gamma| \ll 1$); Δ and Δ_f are the single-pass modulation depths impressed by the amplitude and phase modulators, respectively; m is an integer that defines the harmonic order of the frequency modulation; l is the cavity loss rate; g is the round-trip saturated gain; $\mathcal{D}_g = (2\pi N_g)^{-2}$ is the normalized filtering parameter that accounts for the finite gain bandwidth introduced by a tuning element, such as an etalon, or by the atomic gain line; and N_g is the number of cavity axial modes that fall under the gain line. The saturated gain g obeys the separate rate equation,

$$\frac{\partial g}{\partial T} = -\gamma_{\parallel} \left[g - g_0 + g \int_{-1/2}^{1/2} |\psi(t, T)|^2 dt \right], \quad (1b)$$

where g_0 is the small-signal gain due to the pumping and γ_{\parallel} is the gain relaxation rate normalized to the modulation frequency ($\gamma_{\parallel} \ll 1$). In writing Eq. (1a), we used the weak pulse shaping approximation, assuming that the pulse suffers small changes at each transit in the cavity, and we adopted the simple operator $\mathcal{D}_g\partial^2/\partial t^2$ to account for the finite spectral gain extent of the laser cavity. Different operators can be used, if needed, to more properly account for finite gain bandwidth effects. For instance, if the gain bandwidth were limited by an intracavity etalon, in Eq. (1a) the following change would be in order:

$$\mathcal{D}_g\frac{\partial^2}{\partial t^2} \rightarrow \mathcal{T} \left[-i\frac{1}{T_m}\frac{\partial}{\partial t} \right] - 1, \quad (2a)$$

where

$$\mathcal{T}(\omega) = \frac{1-R}{1-R\exp(2\pi i\omega/\Delta\omega_{FSR})} \simeq \frac{1}{1-i\frac{2\pi R}{1-R}\frac{\omega}{\Delta\omega_{FSR}}} \quad (2b)$$

is the complex transmission function of the etalon, R is the power reflectivity of the etalon facets, and $\Delta\omega_{FSR}$ is the free spectral range of the etalon ($|\omega| \ll \Delta\omega_{FSR}$). Similarly, if the gain bandwidth were limited by the atomic transition line, in Eq. (1a) the operator $\mathcal{D}_g\partial^2/\partial t^2$ should be replaced by $g[\chi(-i(1/T_m)\partial/\partial t) - 1]$, where $\chi(\omega)$ is the normalized complex Lorentzian function of the atomic transition (see, for instance, Ref. [15]). In the following we will mostly use the operator $\mathcal{D}_g\partial^2/\partial t^2$ in the master equation to describe finite gain bandwidth effects, checking that the main effects predicted by the analysis persist also by considering the other above mentioned models. Owing to the cavity boundary conditions, the periodicity condition

$$\psi(-1/2, T) = \psi(1/2, T) \quad (3)$$

has further to be imposed for the pulse envelope.

We note that, when either $\Delta_f = 0$ or $\Delta = 0$, Eq. (1a) reduces to the usual mode-locking models describing AM or FM mode locking, respectively, which have been widely investigated in previous publications. Here we consider the combined effects of amplitude and frequency modulation, the latter providing a continuous frequency shift of the pulse envelope.

B. Eigenmode analysis and pulse splitting bifurcation

The main dynamical properties of the mode-locking regime are determined by the eigenmodes and corresponding eigenvalues of the operator $\mathcal{L}(t)$ entering Eq. (1a); as it will be shown in Sec. IV, the role of the gain dynamics is to force the laser, after transient, to oscillate on the eigenmode with the lowest damping rate. Owing to the periodicity condition (3), the determination of the eigenmodes of the operator \mathcal{L} can be reduced to the calculation of the eigenmodes of a matrix with an infinite dimension, which can be accurately performed by standard numerical routines. Analytical expressions for eigenvalues and eigenmodes in terms of complex-valued Gauss-Hermite polynomials can be derived under a parabolic approximation for both AM and FM terms entering Eq. (1a). Such an analysis, though providing rather approximate results, especially close to bifurcation points, will be developed in the following section and will be useful to understand the bifurcation scenario found in the numerical analysis done in this subsection.

Let us indicate by $\{|n\rangle = \Phi_n(t)\}$ and $\{\lambda_n\}$ the eigenmodes and corresponding eigenvalues of the mode-locking operator \mathcal{L} . Since $\mathcal{L}(t)$ is not self-adjoint, the eigenvalues are in general complex valued. The real part of λ_n , after a sign rever-

sal, represents the loss rate of the eigenmode $|n\rangle$, whereas its imaginary part $\epsilon_n = \text{Im}(\lambda_n)$ corresponds to a slow phase drift that accumulates at successive transits in the cavity. In the following the eigenmodes will be ordered such that $0 \geq \text{Re}(\lambda_n) \geq \text{Re}(\lambda_{n+1})$ ($n=0,1,2,\dots$), i.e., the loss rate increases with the mode order n . In order to transform the differential eigenvalue equation $\mathcal{L}(t)\Phi_n(t) = \lambda_n\Phi_n(t)$ into an algebraic matrix equation, following Eq. (3) we expand the eigenmode $\Phi_n(t)$ in Fourier series by setting $\Phi_n(t) = \sum_{l=-\infty}^{\infty} F_l^{(n)} \exp(2\pi i l t)$; the eigenvalue equation then reduces to the linear algebraic equation $\sum_{s=-\infty}^{\infty} \mathcal{A}_{l,s} F_s^{(n)} = \lambda_n F_l^{(n)}$, where the infinite-dimensional matrix $\mathcal{A}_{l,s}$ is given by [24]

$$\mathcal{A}_{l,s} = \left[-\Delta - 2\pi\gamma i l - \left(\frac{l}{N_g}\right)^2 \right] \delta_{l,s} + \frac{\Delta}{2} (\delta_{l,s+1} + \delta_{l,s-1}) - \frac{\Delta_f}{2} (\delta_{l,s+m} - \delta_{l,s-m}). \quad (4)$$

Notice that the eigenmodes $\{F_l^{(n)}\}$ of the matrix \mathcal{A} represent the spectra of the mode-locking eigenmodes $\{\Phi_n(t)\}$ of $\mathcal{L}(t)$.

We have performed an extended analysis of eigenvalues and eigenmodes of the matrix \mathcal{A} in parameter space by assuming the modulation depth Δ_f of frequency modulation as a control parameter; we typically assumed a zero time detuning ($\gamma=0$), however we checked that the bifurcation scenario observed at $\gamma=0$ persists also by allowing for small detunings (see, e.g., Fig. 3 discussed below). A typical behavior of the eigenvalue spectrum as a function of Δ_f and for a few values of the harmonic order m is shown in Fig. 1. For small values of the modulation depth Δ_f the eigenvalues are real valued and there is one dominant (lowest-order) mode, the $|0\rangle$ mode, which is always a Gaussian-like wave packet centered in correspondence of the minimum of loss modulation cycle, i.e., at $t=0$ [see Fig. 2(a)]. In this case, an increase of the FM depth Δ_f leads to a shift of pulse spectrum from the center of the gain line with a corresponding increase of the loss rate [see Fig. 2(b)]. From the dynamical viewpoint, this case does not show appreciable distinctive aspects as compared to the usual AM mode-locking model without phase modulation; as we will show in Sec. III, for low values of Δ_f the eigenvalue spectrum is fully captured by approximating the frequency modulation term in Eq. (1a) by a *linear* phase term around the pulse position $t=0$, i.e., by neglecting the chirp term induced by the phase modulator. However, as the modulation depth Δ_f is increased above a critical value Δ_{fc} , a qualitative change of the eigenvalue spectrum is observed [25]. Above the critical value Δ_{fc} , the eigenvalue curves in Fig. 1 start to coalesce in pairs, corresponding to the appearance of pairs of complex conjugate eigenvalues (see Fig. 1). The two lowest-order modes, that we indicate by $|0^+\rangle$ and $|0^-\rangle$, have the same loss rate $[\text{Re}(\lambda)]$ but opposite slow frequency shifts $[\text{Im}(\lambda)]$. In the time domain these modes look like chirped Gaussian wave packets whose peaks are slightly and symmetrically displaced from $t=0$ [see Fig. 2(c)]. Furthermore, the sign of the chirp is opposite for the

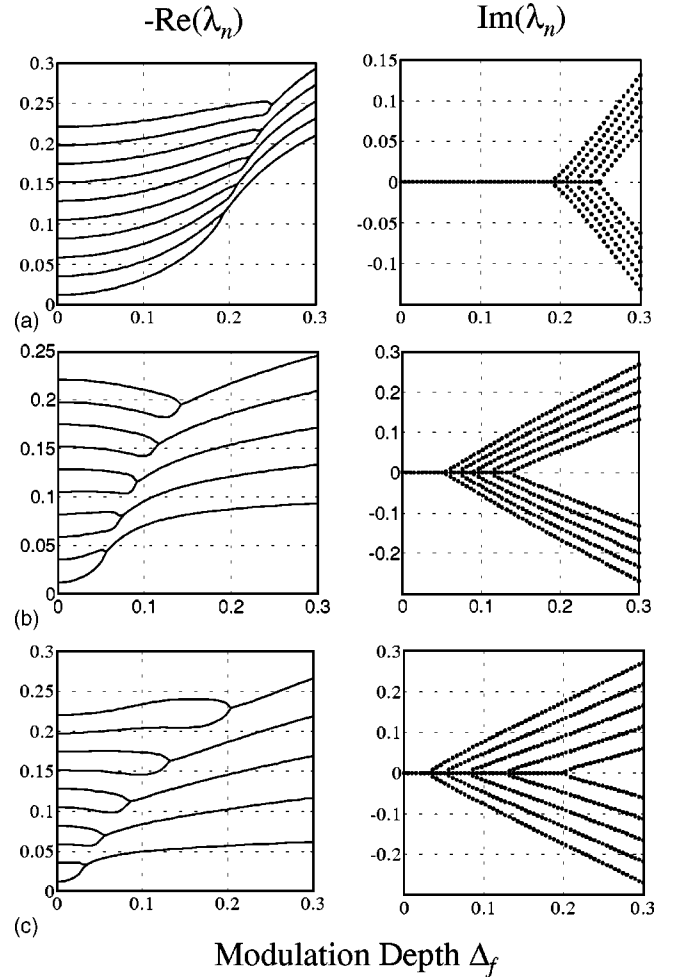


FIG. 1. Behavior of real (left) and imaginary (right) parts of lowest-order eigenvalues λ_n (up to $n=9$) for the mode-locking operator $\mathcal{L}(t)$ versus the depth Δ_f of phase modulation and for a few values of the harmonic order m . (a) $m=2$; (b) $m=4$; (c) $m=6$. The other parameter values are $N_g=60$, $\Delta=1$, and $\gamma=0$.

two modes $|0^+\rangle$ and $|0^-\rangle$. The crossing of the two lowest-order eigenvalue curves near $\Delta_f = \Delta_{fc}$, shown in Fig. 1, will be denoted as a pulse splitting bifurcation, since it will correspond to a splitting of the mode-locked pulse into two slightly displaced and coherently interacting pulses (see Sec. IV). The numerical analysis of the eigenvalue and eigenvector spectra shows that the bifurcation point Δ_{fc} decreases as the harmonic order is increased and, for not too large values of m [25], it scales like $\Delta_{fc} \sim m^{-2}$; in addition, the temporal displacement of the two dominant pulses from $t=0$ is found to slightly increase as Δ_f is increased, with the appearance of a frequency chirp with opposite sign in the two displaced pulses. A detailed explanation of these features will be given in the following section using a Gaussian approximation for the mode-locking eigenmodes. The physical picture of the pulse splitting bifurcation can be nevertheless qualitatively captured by observing that the simultaneous action of amplitude and phase modulations on the pulse produces two competing mechanisms, one of which favors the pulse to be centered close to the minimum of loss modulation, i.e., at $t=0$, and the other one, due to the frequency shifting, which

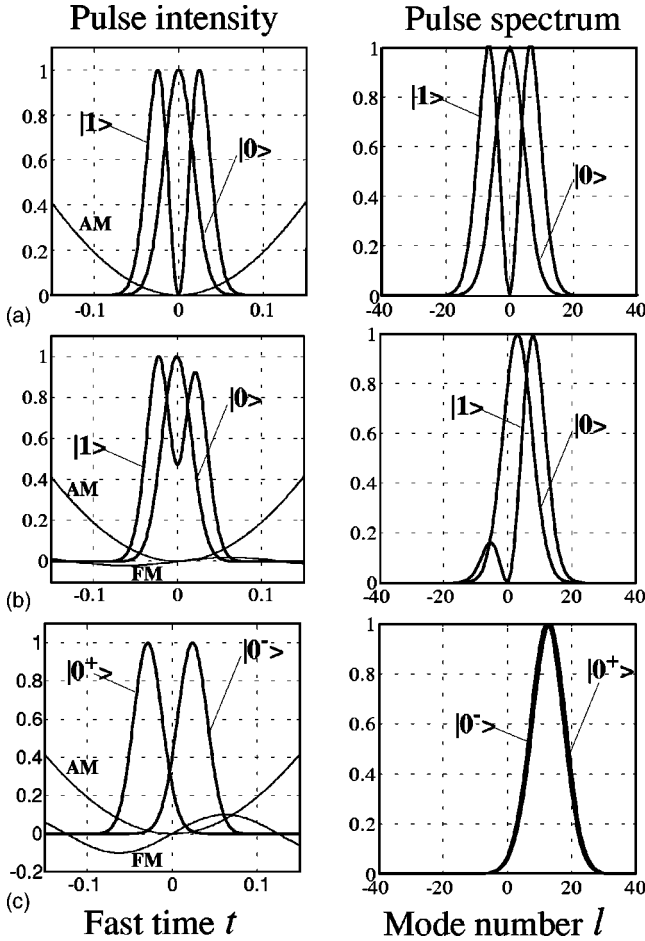


FIG. 2. Behavior of normalized pulse intensity (left) and corresponding spectra (right) for the two lowest-order modes for increasing values of modulation depth Δ_f : (a) $\Delta_f=0$; (b) $\Delta_f=0.02$; (c) $\Delta_f=0.1$. The other parameter values are: $m=4$, $N_g=60$, $\Delta=1$, and $\gamma=0$, corresponding to $\Delta_{fc}\approx 0.055$ [see Fig. 1(b)]. The thin curves in the left plots represent the loss (AM) and phase (FM) modulation profiles.

tends to push the pulse far away from $t=0$ in either directions. The former mechanism is merely due to the loss modulation dynamics, whereas the latter one arises from the phase modulation term which, close to $t=0$, varies linearly with time, producing a continuous frequency drift of the pulse spectrum at successive transits. This continuous frequency drift causes the pulse spectrum to move far away from the center of the spectral gain band, thus increasing the pulse loss. As the pulse center is shifted *in time* away from $t=0$, the frequency drift is reduced and tends to vanish close to $t = \pm T_m/(2m)$, where the phase modulation has two stationary points. Since the rate of the frequency drift is proportional to the modulation depth Δ_f , for sufficiently high phase modulation strengths the loss mechanism introduced by the spectral pulse drift may become dominant over the loss modulation, leading to the pulse splitting bifurcation. We note that the competition between these two mechanisms persists also in presence of a slight detuning between the modulation frequency ω_m and the cavity free spectral range $\Delta\omega_{ax}$, i.e., for $\gamma \neq 0$, or using in Eq. (1a) a different model

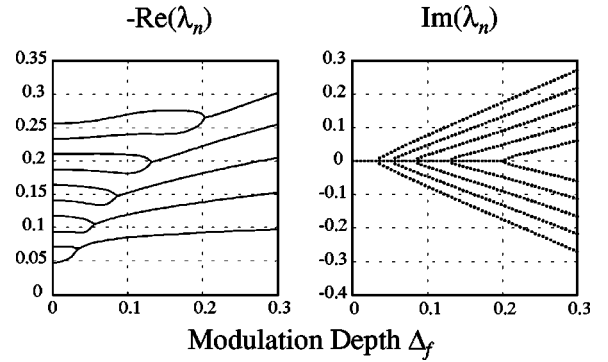


FIG. 3. Behavior of real (left) and imaginary (right) parts of lowest-order eigenvalues λ_n (up to $n=9$) for the mode-locking operator $\mathcal{L}(t)$ in case of nonzero detuning. Parameter values are the same as in Fig. 1(c) except for $\gamma=1 \times 10^{-3}$.

for the spectral gain bandwidth. As an example, in Fig. 3 it is plotted the eigenvalue spectrum in case of a nonzero detuning, showing the persistence of eigenvalue crossing and of the pulse splitting bifurcation.

III. GAUSSIAN PULSE ANALYSIS

The determination of the eigenvalue spectrum and the corresponding eigenvectors for the mode-locking operator \mathcal{L} , as given in Eq. (1a), requires in general a direct numerical analysis. Nevertheless, if the mode-locked pulses are assumed to be well localized somewhere, with a duration much shorter than T_m/m , the sinusoidal AM and FM terms entering the expression of $\mathcal{L}(t)$ may be expanded up to second order in time, leading to an expression for $\mathcal{L}(t)$ which is linear in $\partial^2/\partial t^2$, $\partial/\partial t$, t , and t^2 . For such an operator, the eigenvalues and corresponding eigenmodes can be determined analytically in terms of complex Hermite-Gaussian modes (see, for instance, Ref. [26]). In order to properly describe the pulse splitting bifurcation found in the numerical analysis, the pulse center of mass t_0 has to be left undetermined at this stage. We thus expand the AM and FM terms entering Eq. (1a) up to second order in $t-t_0$, yielding

$$\mathcal{L}(t) = -\gamma \frac{\partial}{\partial t} + D_g \frac{\partial^2}{\partial t^2} + \beta_2 (t-t_0)^2 + \beta_1 (t-t_0) + \beta_0, \quad (5)$$

where the coefficients β_0 , β_1 , and β_2 are given by

$$\beta_0 = -\Delta [1 - \cos(2\pi t_0)] - i\Delta_f \sin(2\pi m t_0), \quad (6a)$$

$$\beta_1 = -2\pi\Delta \sin(2\pi t_0) - 2\pi i m \Delta_f \cos(2\pi m t_0), \quad (6b)$$

$$\beta_2 = -2\pi^2\Delta \cos(2\pi t_0) + 2\pi^2 i m^2 \Delta_f \sin(2\pi m t_0). \quad (6c)$$

The eigenvalue equation $\mathcal{L}(t)|n\rangle = \lambda_n|n\rangle$ can be satisfied assuming for $|n\rangle$ a complex Hermite-Gaussian mode of the form [26]

$$|n\rangle = H_n(\xi t + \rho) \exp[-\alpha(t-t_0)^2 + i\beta(t-t_0)], \quad (7)$$

where $\alpha = \alpha_R + i\alpha_I$ is the complex-valued Gaussian pulse parameter defining pulse duration and pulse chirp ($\alpha_R > 0$); β is a real-valued parameter that determines the pulse frequency shift; and $H_n(x)$ is the Hermite polynomial of order n with complex argument $x = \xi t + \rho$, where ξ and ρ are complex-valued parameters. The pulse parameters α_R , α_I , β , ξ , and ρ entering the ansatz (7), as well as the pulse position t_0 , have to be determined by substitution of Eq. (7) into the eigenvalue equation $\mathcal{L}(t)|n\rangle = \lambda_n|n\rangle$ and imposing that the resulting equation for H_n reduces to the differential equation of Hermite polynomials, i.e., $d^2H_n/dx^2 - 2xdH_n/dx + 2nH_n = 0$. Using Eqs. (5) and (6), after some cumbersome but straightforward calculations one obtains the following expressions for the eigenvalues λ_n and parameters ξ and ρ :

$$\lambda_n = \lambda_0 - 4\alpha\mathcal{D}_g n \quad (n=1,2,3,\dots), \quad (8a)$$

$$\lambda_0 = -\mathcal{D}_g(2\alpha + \beta^2) - i\beta\gamma + \Delta\cos(2\pi t_0) - \Delta - i\Delta_f\sin(2\pi m t_0), \quad (8b)$$

$$\xi = \sqrt{2\alpha}, \quad \rho = \frac{\gamma - 2i\beta}{2\sqrt{2\alpha}} - \sqrt{2\alpha}t_0, \quad (9)$$

where α , β , and t_0 are the solutions of the following coupled equations:

$$2\gamma\alpha - 4i\alpha\beta\mathcal{D}_g - 2\pi\Delta\sin(2\pi t_0) - 2\pi im\Delta_f\cos(2\pi m t_0) = 0, \quad (10a)$$

$$4\alpha^2\mathcal{D}_g - 2\pi^2\Delta\cos(2\pi t_0) + 2\pi^2 im^2\Delta_f\sin(2\pi m t_0) = 0. \quad (10b)$$

Since the pulse parameters α , β , and t_0 do not depend on the mode order n , Eq. (8a) clearly shows that the mode loss rate $-\text{Re}(\lambda_n)$ increases with the mode order n , and thus the lowest-order mode, attained at $n=0$, corresponds always to a Gaussian pulse, which is in general chirped ($\alpha_I \neq 0$) and shifted in frequency from the center of the spectral gain curve ($\beta \neq 0$). In addition, the coupled equations (10a) and (10b), which define the pulse parameters and pulse position, may admit multiple solutions leading to different loss rates through Eq. (8b). Such a multiplicity is indeed responsible for the eigenvalue crossing and pulse splitting bifurcation found in the numerical analysis of Sec. II. To simplify our analysis, let us consider the case of zero detuning, i.e., let us assume $\gamma=0$. In this case, after setting $\alpha = \alpha_R + i\alpha_I$, from Eqs. (10a) and (10b) the following equations for the real-valued pulse parameters α_R , α_I , t_0 , and β are derived:

$$2\pi m\Delta_f\cos(2\pi m t_0) = -4\beta\mathcal{D}_g\alpha_R, \quad (11a)$$

$$2\pi m\Delta_f\sin(2\pi m t_0) = -\frac{8\mathcal{D}_g\alpha_R\alpha_I}{m\pi}, \quad (11b)$$

$$2\pi\Delta\sin(2\pi t_0) = 4\beta\mathcal{D}_g\alpha_I, \quad (11c)$$

$$2\pi\Delta\cos(2\pi t_0) = \frac{4(\alpha_R^2 - \alpha_I^2)\mathcal{D}_g}{\pi}. \quad (11d)$$

Equations (11) always admit of a solution corresponding to a pulse centered at $t_0=0$ without chirp ($\alpha_I=0$); for such a solution one has

$$t_0 = 0, \quad (12a)$$

$$\alpha_I = 0, \quad (12b)$$

$$\alpha_R = \pi\sqrt{\frac{\Delta}{2\mathcal{D}_g}}, \quad (12c)$$

$$\beta = -\frac{m\Delta_f}{\sqrt{2\Delta\mathcal{D}_g}}, \quad (12d)$$

leading to a real eigenvalue [see Eq. (8b)],

$$\lambda_0 = -\pi\sqrt{2\Delta\mathcal{D}_g} - \frac{m^2\Delta_f^2}{2\Delta}. \quad (13)$$

Notice that in absence of the phase modulation ($\Delta_f=0$), this solution reduces to the usual Gaussian pulse of AM mode-locked lasers, with a pulse duration determined by the laser gain bandwidth through Eq. (12c); the presence of a phase modulation ($\Delta_f \neq 0$) merely produces a shift of the pulse spectrum from the center of the gain line ($\beta \neq 0$) by an amount which is proportional to the strength of the phase modulation [see Eq. (12d)]; the pulse spectrum shift produces a corresponding increase of the loss rate [see Eq. (13)], despite pulse position and pulse duration not being influenced by the phase modulation. However, for sufficiently high values of the modulation depth Δ_f , the coupled equations (11) admit of a solution corresponding to a chirped pulse with $t_0 \neq 0$, i.e., to a pulse which is detuned in time from the minimum of loss modulation. Notice also that since Eqs. (11) are invariant under the change $t_0 \rightarrow -t_0$ and $\alpha_I \rightarrow -\alpha_I$, time-detuned pulse solutions appear always in pairs, symmetrically displaced from $t=0$, and with opposite sign of chirp α_I . In addition, from Eq. (8b) it follows that these two companion solutions have the same loss rate $-\text{Re}(\lambda_0)$ but opposite values of $\text{Im}(\lambda_0)$. The time displacement t_0 can be found as a root of the following transcendental equation:

$$\sin(2\pi m t_0) \left[\frac{m^3\Delta_f^2 \cos(2\pi m t_0)}{2\Delta^2 \sin(2\pi t_0)} - \frac{m}{2} \frac{\sin(2\pi t_0)}{\cos(2\pi m t_0)} \right] = \cos(2\pi t_0). \quad (14)$$

In correspondence, the pulse parameters are given by

$$\alpha_R = \sqrt{\frac{\pi^2 m^3 \Delta_f^2 \sin(4\pi m t_0)}{8\Delta\mathcal{D}_g \sin(2\pi t_0)}}, \quad (15a)$$

$$\alpha_I = \pm \sqrt{\frac{\pi^2 m \Delta \sin(2\pi m t_0) \sin(2\pi t_0)}{4\mathcal{D}_g \cos(2\pi m t_0)}}, \quad (15b)$$

$$\beta = -\sqrt{\frac{\Delta \cos(2\pi m t_0) \sin(2\pi t_0)}{m\mathcal{D}_g \sin(2\pi m t_0)}}. \quad (15c)$$

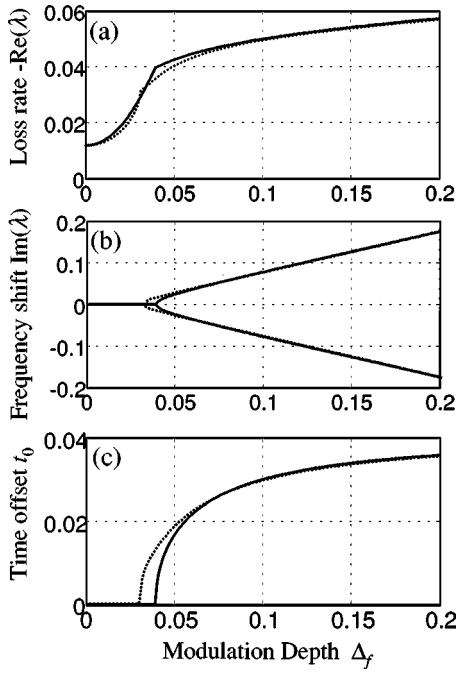


FIG. 4. Behavior of loss rate (a), slow frequency shift (b), and time displacement (c) versus modulation depth Δ_f for the lowest-order pulse mode as calculated by the Gaussian pulse analysis (solid curves) and by the eigenvector computation of mode-locking matrix \mathcal{A} (dotted curves). Parameter values are: $N_g = 60$, $\Delta = 1$, $m = 6$, and $\gamma = 0$.

Equation (14) leads to acceptable pulse solutions provided that the modulation depth Δ_f is larger than a critical value Δ_{fc} ; when Δ_f approaches Δ_{fc} from above, t_0 goes to zero, thus recovering the solution given by Eqs. (12). The value of Δ_{fc} is found by setting $t_0 = 0$ in Eq. (14) and reads

$$\Delta_{fc} = \frac{\sqrt{2}\Delta}{m^2}. \quad (16)$$

For $\Delta_f > \Delta_{fc}$, the loss rate $-\text{Re}(\lambda_0)$ for the displaced solutions, as obtained from Eq. (8b) using Eqs. (14) and (15), turns out to be smaller than that given by Eq. (13). The value Δ_{fc} thus provides an estimate of the bifurcation point connecting the unchirped and centered Gaussian pulse solution $|0\rangle$, found at low values of Δ_f , with the chirped and time-displaced Gaussian pulse solutions $|0^+\rangle$ and $|0^-\rangle$ found at larger values of Δ_f and discussed in the preceding section. As an example, in Fig. 4 we show the behavior of the loss rate, slow frequency shift, and time displacement for the lowest-order Gaussian mode as computed from the approximate Gaussian pulse analysis [Eqs. (8b) and (10)] and by a direct numerical analysis as in Sec. II. Note that the approximate Gaussian pulse analysis provides a good fit to the full numerical curves, apart for a small region around the bifurcation point. Moreover, the dependence of the bifurcation point Δ_{fc} on the harmonic order m , as given in Eq. (16), is in good agreement with the numerical results.

IV. PULSE DYNAMICS

In the previous sections we have determined the properties of the mode-locking operator $\mathcal{L}(t)$, revealing the existence of eigenvalue coalescing as the modulation depth Δ_f is increased, which corresponds to the emergence of two dominant pulse states symmetrically displaced in time from the minimum of loss modulation. In this section we study both analytically and numerically the dissipative pulse dynamics by taking into account the role of the gain variable and describe in detail the onset of FM-induced pulse slitting.

A. Pulse splitting and gain dynamics: Eigenmode expansion analysis

The dynamics leading to the formation of a steady-state mode-locking regime is provided by the mechanism of gain saturation, which is ruled by Eq. (1b). To study the evolution of an arbitrary initial field distribution $\psi_0(t)$ at successive transits in the cavity, it is convenient to expand the field envelope $\psi(t, T)$ in series of the eigenmodes $|n\rangle = \Phi_n(t)$ of the mode-locking operator $\mathcal{L}(t)$, which we assume to be a complete set of functions with respect to the variable t . We then set

$$\psi(t, T) = \sum_n f_n(T) \Phi_n(t), \quad (17)$$

where the coefficients f_n in the expansion depend on the round-trip variable T . In order to determine the equations of motion for these coefficients, let us indicate by $|n^\dagger\rangle = \Phi_n^\dagger(t)$ the eigenmode of the adjoint mode-locking operator, $\mathcal{L}^\dagger(t)$, with eigenvalue λ_n^* . The set of functions $|n\rangle$ and $|n^\dagger\rangle$ are hence orthogonal, and we assume a normalization such that $\langle m^\dagger | n \rangle = \int_{-1/2}^{1/2} dt \Phi_m^*(t) \Phi_n(t) = \delta_{m,n}$ and $\langle n | n \rangle = \int_{-1/2}^{1/2} dt \Phi_n^*(t) \Phi_n(t) = 1$ [27]. Substituting expansion (17) into Eq. (1a), multiplying both sides of the equation so obtained by $\Phi_m^\dagger(t)$, and integrating over the fast time variable t , one then obtains the following equations for the coefficients $f_m(T)$:

$$\frac{df_m}{dT} = (g - l + \lambda_m) f_m, \quad (18)$$

with the initial conditions $f_m(0) = \langle m^\dagger | \psi_0 \rangle$. The equation for the gain dynamics [Eq. (1b)] then reads

$$\frac{dg}{dt} = -\gamma \left(g - g_0 + g \sum_{m,n} K_{m,n} f_m^* f_n \right), \quad (19)$$

where we have set $K_{m,n} = \langle m | n \rangle$ ($K_{n,n} = 1$, $K_{m,n} = K_{n,m}^*$). The formal integration of Eqs. (18) allows one to write

$$f_n(T) = f_0(T) \frac{f_n(0)}{f_0(0)} \exp[(\lambda_n - \lambda_0)T]. \quad (20)$$

If we assume that $\Delta_f < \Delta_{fc}$, there is one dominant mode with real eigenvalue λ_0 , i.e., $\text{Re}(\lambda_n) < \lambda_0$ for $n = 1, 2, 3, \dots$, so that

after an initial transient one has $f_n(T) \approx 0$ for $n \geq 1$, and the dynamics is merely described by the following two coupled equations for f_0 and g :

$$\frac{df_0}{dT} = (g - l - q)f_0, \quad (21a)$$

$$\frac{dg}{dT} = -\gamma_{\parallel}(g - g_0 + g|f_0|^2), \quad (21b)$$

where $q = -\text{Re}(\lambda_0)$ is the loss rate of dominant Gaussian mode. These equations admit of the stationary solution $g = l + q$ and $|f_0|^2 = g_0 / (l + q) - 1$ for $g_0 > g_{th} = l + q$, corresponding to a steady-state mode-locked pulse operation.

For $\Delta_f > \Delta_{fc}$, there are two dominant eigenmodes with the same loss rate $q = -\text{Re}(\lambda_0) = -\text{Re}(\lambda_1)$ and opposite slow frequency shift $\epsilon = \text{Im}(\lambda_0) = -\text{Im}(\lambda_1)$; these modes were indicated by $|0^+\rangle$ and $|0^-\rangle$ in Sec. II. In this case, from Eq. (20) after transient one obtains $f_n(T) \approx 0$ for $n \geq 2$,

$$f_1(T) = f_0(T) \frac{f_1(0)}{f_0(0)} \exp(-2i\epsilon T), \quad (22)$$

and the dynamics is described by the following two coupled equations for f_0 and g :

$$\frac{df_0}{dT} = (g - l - q)f_0 + i\epsilon f_0, \quad (23a)$$

$$\frac{dg}{dT} = -\gamma_{\parallel} \{ g - g_0 + g [1 + |\Lambda|^2 + 2|K_{0,1}||\Lambda| \cos(2\epsilon T - \phi)] |f_0|^2 \}, \quad (23b)$$

where we have set $\Lambda \equiv f_1(0)/f_0(0)$ and $\phi \equiv \text{Im}\{\ln(K_{0,1}\Lambda)\}$. We note that since \mathcal{L} is not self-adjoint [27], one has $|K_{0,1}| \neq 0$, so that the dynamics given by Eqs. (23a) and (23b) is nonautonomous and the solution $f_0(T), g(T)$ is attracted toward a limit cycle. The mode-locked pulse is now given by the superposition of the two displaced pulse modes $\Phi_0(t)$ and $\Phi_1(t)$ according to

$$\psi(t, T) = f_0(T) [\Phi_0(t) + \Lambda \Phi_1(t) \exp(-2i\epsilon T)]. \quad (24)$$

Equation (24) shows that the mode-locked pulse varies periodically with the round-trip number T with a period given by π/ϵ , and its shape is determined by the coherent interference of the two displaced pulse eigenmodes $\Phi_0(t)$ and $\Phi_1(t)$ with a relative amplitude equal to Λ , which depends on the initial conditions. In particular, if we assume $\gamma = 0$ and use the parabolic approximation for the mode-locking operator $\mathcal{L}(t)$, one has

$$\Phi_0(t) = \left(\frac{\pi}{2\alpha_R} \right)^{1/4} \exp[-\alpha(t - t_0)^2 + i\beta(t - t_0)], \quad (25)$$

$$\Phi_1(t) = \left(\frac{\pi}{2\alpha_R} \right)^{1/4} \exp[-\alpha^*(t + t_0)^2 + i\beta(t + t_0)], \quad (26)$$

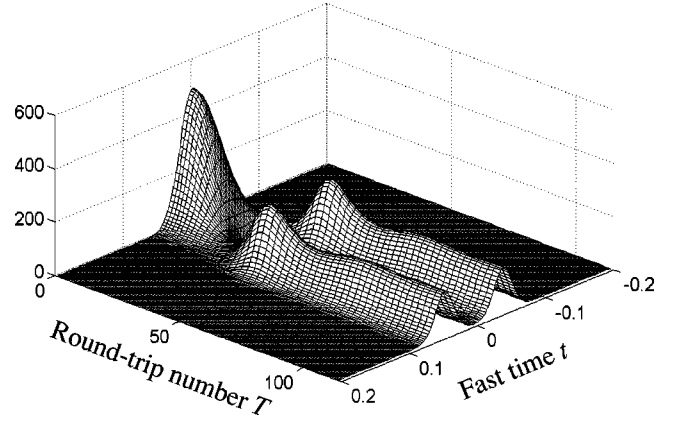


FIG. 5. Evolution of the mode-locked pulse intensity $|\psi(t, T)|^2$ at successive transits in the cavity after switching on of the phase modulator at $T=0$. Parameter values are $\Delta=1$, $m=5$, $N_g=50$, $\Delta_f=0.3$, $\gamma=0$, $\gamma_{\parallel}=0.01$, $l=0.05$, $g_0/l=1.5$.

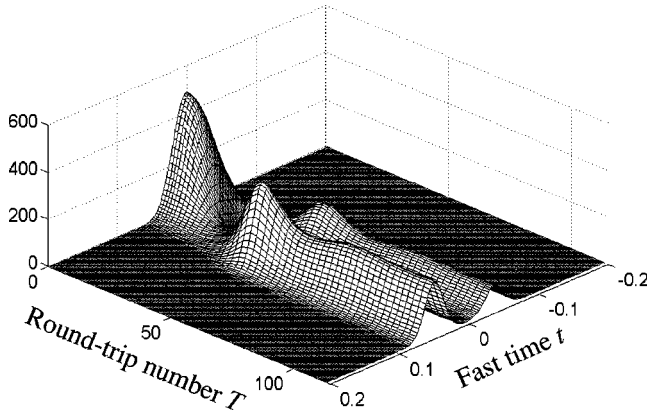
where t_0 , $\alpha = \alpha_R + i\alpha_I$, and β are given by Eqs. (14) and (15), and

$$|K_{0,1}| = \frac{\pi}{2} \frac{1}{\sqrt{\alpha_R|\alpha|}} \exp(-2\alpha_R t_0^2). \quad (27)$$

In order to understand the onset of the pulse splitting dynamics, let us suppose that the phase modulator is initially switched off ($\Delta_f=0$) and the AM mode-locked laser oscillates on the steady-state Gaussian pulse centered at $t=0$. As the phase modulator is suddenly switched on with a modulation depth larger than Δ_{fc} , after a transient the pulse envelope $\psi(t, T)$ is attracted toward Eq. (24) with $|\Lambda|=1$, i.e., a pulse splitting takes place, corresponding to the coherent oscillation of the two displaced pulse modes $|0^+\rangle$ and $|0^-\rangle$ according to Eq. (24). An example of pulse splitting induced by the application of a steplike FM signal to the AM mode-locked laser is shown in Fig. 5, where the evolution of pulse intensity $|\psi(t, T)|^2$ at successive round trips, as obtained by a direct numerical simulation of Eqs. (1) and (3), is reported. We note that an unbalanced excitation of the two displaced pulses ($|\Lambda| \neq 1$) may break the symmetric splitting behavior shown in Fig. 5. Such a situation occurs, for instance, when $\gamma \neq 0$ or when the spectral gain model given by Eqs. (2a) and (2b) is used. A detailed numerical analysis of these cases is given in the following subsection.

B. Numerical results

A direct investigation of the pulse dynamics for the AM mode-locked laser with frequency shifting has been performed by numerical integration of Eqs. (1) and (3) under different operational conditions. The integration was typically done in the spectral domain by numerical integration of a set of ordinary differential equations obtained by discretizing the mode-locking operator \mathcal{L} as in Sec. II B and accounting for the gain dynamics. After introducing the expansion $\psi(t, T) = \sum_n F_n(T) \exp(2\pi i n t)$, these equations read explicitly

FIG. 6. Same as Fig. 5 but with $\gamma=1 \times 10^{-4}$.

$$\frac{dF_n}{dT} = (g-l)F_n + \sum_l \mathcal{A}_{n,l} F_l \quad (n=0, \pm 1, \pm 2, \dots), \quad (28a)$$

$$\frac{dg}{dT} = -\gamma_{\parallel} \left(g - g_0 + g \sum_n |F_n|^2 \right), \quad (28b)$$

where the mode-locking matrix \mathcal{A} is given by Eq. (4) [24]. Equations (28) have been integrated using an accurate variable-step fourth-order Runge-Kutta method with different initial conditions and including a sufficient number of modes in the expansion to safely accommodate the entire spectrum of the mode-locked pulse during its evolution.

We first integrated Eqs. (28) starting from a small random noise with the phase modulator switched off, so that after a fast transient the stationary mode-locked pulse of the AM mode-locking regime is attained. At $T=0$ we then suddenly switched on the phase modulator, and recorded the evolution of the pulse intensity at successive transits in the cavity. Figures 5 and 6 show typical behaviors of such a pulse evolution for a zero (Fig. 5) and for a nonzero (Fig. 6) detuning parameter γ . In both cases a pulse splitting is observed after the FM switch is on, however in the detuned case the two pulses have different peak intensities. The reason thereof is that the parameter Λ , entering Eq. (24) and defining the relative amplitude of the two displaced pulses, depends on the

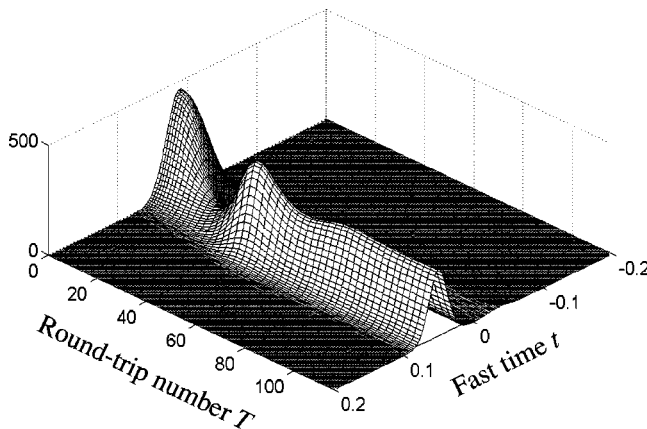
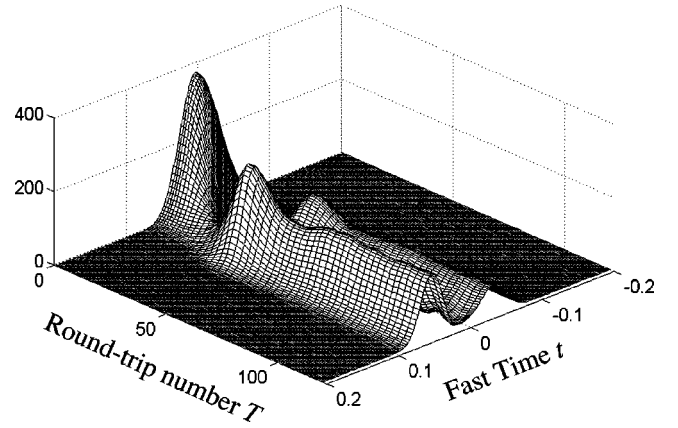
FIG. 7. Same as Fig. 5 but with $\gamma=4 \times 10^{-4}$.

FIG. 8. Same as Fig. 5, but for a spectral filtering simulated using the transmission function of an etalon [see Eqs. (2a) and (2b)]. Parameter values for the etalon are: $R=0.9$, $\Delta\omega_{FSR}/\omega_m=2000$, and $\gamma=0.0045$; the other parameter values are as in Fig. 5. The value of γ has been chosen to compensate for the linear dispersive part of the etalon spectral function [see Eq. (2b)].

initial condition according to $\Lambda = \langle \Phi_1^\dagger | \psi_0 \rangle / \langle \Phi_0^\dagger | \psi_0 \rangle$, where $\psi_0(t)$ is the AM mode-locked pulse at $T=0$. In case of zero detuning the projections of the mode-locked pulse $\psi_0(t)$ onto the two adjoint eigenmodes $\Phi_1^\dagger(t)$ and $\Phi_2^\dagger(t)$ yield the same value, however in the detuned case this is not the case, leading to $|\Lambda| \neq 1$. At increasing values of γ , Λ may vanish, leading eventually to the disappearance of the pulse splitting (see Fig. 7). We also checked that the pulse splitting bifurcation persists by assuming a different model to account for the finite spectral gain bandwidth of the cavity, as discussed in Sec. II A. As an example, in Fig. 8 we show the occurrence of pulse splitting by assuming an intracavity etalon as a spectral selective element. In order to understand the asymmetry of splitting in the figure, let us notice that in this case the dispersive properties introduced by the etalon spectral function [Eq. (2b)], despite to slightly change the cavity free spectral range of the bared cavity, also slightly affect the shape and offset of the two displaced chirped pulses, making again $|\Lambda| \neq 1$ in Eq. (24).

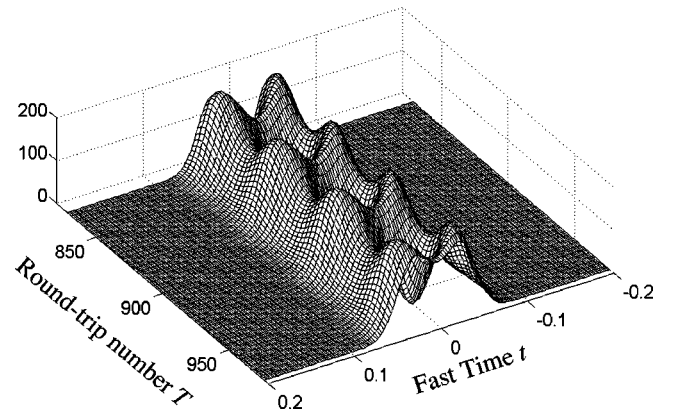


FIG. 9. Periodic two-pulse coherent dynamics after transient laser switch on at $T=0$. Parameter values are $\Delta=1$, $m=5$, $N_g=50$, $\Delta_f=0.1$, $\gamma=0$, $\gamma_{\parallel}=10^{-3}$, $l=0.05$, $g_0/l=1.5$.

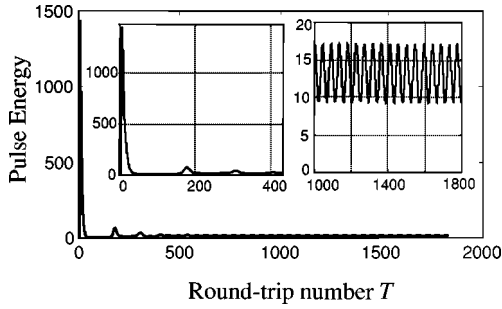


FIG. 10. Behavior of pulse energy, $\int_{-1/2}^{1/2} dt |\psi(t, T)|^2$, versus round-trip number, showing the onset of transient relaxation oscillations after laser switch on (inset on the left side) and periodic oscillations due to the coherent two-pulse dynamics after transient (inset on the right side). Parameter values are as in Fig. 9.

Finally, we integrated Eqs. (28) assuming that *both* AM and FM signals are zero at $T < 0$, and that they are simultaneously switched on at $T = 0$. For $\Delta_f > \Delta_{fc}$, after an initial transient the mode-locked pulse undergoes a periodic evolution, with a period equal to $\approx \pi/\epsilon$ as predicted by the eigenvalue analysis, showing a periodic pattern that results from the interference of the two displaced pulses according to Eq. (24). We note that if the pulse displacement is comparable with the pulse duration, the interference pattern leads to a considerable pulse reshaping rather than pulse splitting; an example of such a periodic pattern is shown in Fig. 9. The transient switch on of the AM and FM signals also leads to the transient excitation of laser relaxation oscillations, as shown in Fig. 10.

As a practical example, let us consider a Nd:yttrium aluminum garnet (YAG) laser (gain bandwidth ≈ 126 GHz at 300 K, gain relaxation rate ≈ 4.35 kHz) AM mode locked at a repetition frequency $\nu_m = 1/T_m = 100$ MHz, and assume that the gain bandwidth of the cavity is determined by an intracavity thin etalon with a free spectral range $\Delta\nu_{FSR} \approx 200$ GHz and coated facets with reflectivity $R \approx 90\%$. A transmission peak of the etalon is assumed to be tuned at the center of the atomic gain line at 1064 nm. Assuming $\Delta \approx 0.1$, $m = 5$, $\Delta_f \approx 0.03$, and $\gamma = 0.0045$, one obtains for the modes $|0^+\rangle$ and $|0^-\rangle$ a duration (full width at half maximum) of ≈ 701 ps and 735 ps, respectively, with a time displacement t_0 , from $t = 0$, given by ≈ 475 ps and ≈ 375 ps for the two pulses, respectively. Furthermore, the periodicity due to coherent pulse dynamics, given by π/ϵ , is about 179 round-trip numbers, corresponding to ≈ 1.79 μs . Figure 11 shows the coherent two-pulse dynamics of the mode-locked pulse train as obtained after relaxation oscillation transient, assuming $l = 0.05$, $g_0/l = 1.3$, and $\gamma_{\parallel} = 4.35 \times 10^{-5}$.

V. CONCLUSIONS AND DISCUSSION

We have analyzed the dynamical behavior of the classic loss-modulated mode-locked laser model [3] in presence of simultaneous frequency shift provided by an intracavity phase modulator, and found a pulse splitting bifurcation in-

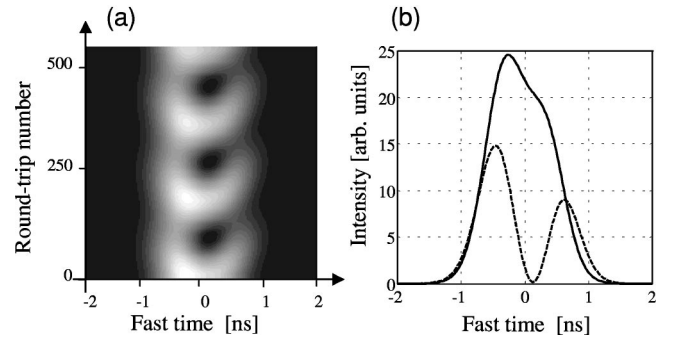


FIG. 11. (a) Behavior of pulse intensity versus round-trip number after transient for the Nd:YAG mode-locked laser model discussed in the text. (b) Detailed intensity pulse profiles taken at $T = 0$ (solid line) and at $T = 80$ (dashed line). The value of γ has been chosen to compensate for the linear dispersive part of the etalon spectral function [see Eq. (2b)].

duced by the phase perturbation. At low values of phase modulation depth, the mode-locked pulse is single peaked with a peak position locked at the minimum of loss modulation but with a spectrum which is shifted away from the center of the gain line due to continuous frequency sliding. However, as the modulation depth is increased above a threshold value, a pulse splitting bifurcation is observed, which leads to the coherent oscillation of two chirped wave packets, symmetrically displaced in time from the minimum of loss modulation (see Figs. 5, 6, and 8). Since the two wave packets are slightly shifted in frequency [$\text{Im}(\lambda_0) = -\text{Im}(\lambda_1)$], their interference leads to a periodic intensity pattern during successive round trips (see Figs. 9 and 11). This feature bears a close connection with the periodic dynamical behavior found in conservative systems involving the interference of two modes, such as periodic power exchange in two coupled waveguides [21] or quantum tunneling of a wave packet in a double-well potential [20], where the periodic dynamics is due to frequency splitting of the two symmetric and antisymmetric supermodes. As a final remark, we point out that the pulse splitting behavior found in our mode-locking model provides an example of wave packet dichotomy in a Schrödinger-like *dissipative* dynamical system and it is thus rather different from the wave packet splitting dynamics encountered in other *conservative* dynamical systems. In particular, the classic wave packet splitting found for Schrödinger wave packets in a single-well potential, such as the dichotomy of the wave function of a bound electron in a strong laser field [22] or the splitting of a Bose-Einstein condensate in a periodically shaken trap [23], occurs in presence of a time-dependent periodic potential. In such case the wave packet splitting arises due to a nonadiabatic effect: when the time scale of the shaking is shorter than the other relevant time scales of the system, the time-periodic potential can be replaced by its time average, and the wave packet splitting results from the existence of a double well in the averaged potential. Conversely, in our model wave packet splitting is of purely dissipative nature and does not require any nonautonomous dynamics.

- [1] D.J. Kuizenga and A.E. Siegman, *IEEE J. Quantum Electron.* **6**, 694 (1970).
- [2] N.P. Barnes, *J. Appl. Phys.* **45**, 1291 (1974).
- [3] H.A. Haus, *IEEE J. Quantum Electron.* **11**, 323 (1975).
- [4] G.H.C. New, *Rep. Prog. Phys.* **46**, 877 (1983).
- [5] U. Morgner and F. Mitschke, *Phys. Rev. E* **58**, 187 (1998).
- [6] F.X. Kärtner, D.M. Zumbühl, and N. Matuschek, *Phys. Rev. Lett.* **82**, 4428 (1999).
- [7] S. Longhi and P. Laporta, *Phys. Rev. E* **61**, R989 (2000).
- [8] H.J. Eichler, *Opt. Commun.* **56**, 351 (1986).
- [9] P. Kean, K. Smith, and W. Sibbet, *Opt. Commun.* **61**, 129 (1987).
- [10] Y.M. Jhon and H.J. Kong, *IEEE J. Quantum Electron.* **29**, 1042 (1999).
- [11] O. Haderka and P. Maly, *J. Mod. Opt.* **41**, 927 (1994).
- [12] H.J. Eichler, I.G. Koltchanov, and B. Liu, *Appl. Phys. B: Lasers Opt.* **B61**, 81 (1995).
- [13] L. Trefethen, A. Trefethen, S.C. Reddy, and T. Driscoll, *Science* **261**, 578 (1993).
- [14] S.E. Harris and O.P. McDuff, *IEEE J. Quantum Electron.* **1**, 245 (1965).
- [15] S. Longhi and P. Laporta, *Phys. Rev. A* **60**, 4016 (1990).
- [16] B.F. Farrell and P.J. Ioannou, *Phys. Rev. Lett.* **72**, 1188 (1994).
- [17] A.E. Siegman, *Appl. Phys. B: Lasers Opt.* **B60**, 247 (1995).
- [18] U. Peschel, T. Pertsch, and F. Lederer, *Opt. Lett.* **23**, 1701 (1998); G. Lenz, I. Talanina, and C.M. de Sterke, *Phys. Rev. Lett.* **83**, 963 (1999); R. Morandotti, U. Peschel, J.S. Aitchison, H.S. Eisenberg, and Y. Silberberg, *ibid.* **83**, 4756 (1999); T. Pertsch, P. Dannberg, W. Elflein, A. Bräuer, and F. Lederer, *ibid.* **83**, 4752 (1999);
- [19] S. Longhi, *Phys. Rev. E* **63**, 037201 (2001); **64**, 047201 (2001).
- [20] L.D. Landau and E.M. Lifshitz, *Quantum Mechanics* (Pergamon Press, Oxford, 1964), p. 177.
- [21] See, for instance, A. Yariv, *Quantum Electronics* (Wiley, New York, 1989), p. 631.
- [22] M. Pont, N.R. Walet, M. Gavrilă, and C.W. McCurdy, *Phys. Rev. Lett.* **61**, 939 (1988).
- [23] R. Dum, A. Sanpera, K.-A. Suominen, M. Brewczyk, M. Kus, K. Rzazewski, and M. Lewenstein *Phys. Rev. Lett.* **80**, 3899 (1998).
- [24] We note that if the filtering element in the cavity is provided by an etalon and the replacement given by Eq. (2a) is made in Eq. (1a), the elements of the mode-locking matrix \mathcal{A} would change according to the following equation:
- $$\mathcal{A}_{l,s} = \left[-\Delta - 2\pi\gamma il + \frac{1-R}{1-R\exp(2\pi il\omega_m/\Delta\omega_{FSR})} - 1 \right] \delta_{l,s} + \frac{\Delta}{2}(\delta_{l,s+1} + \delta_{l,s-1}) - \frac{\Delta_f}{2}(\delta_{l,s+m} - \delta_{l,s-m}).$$
- [25] The bifurcation from real-valued eigenvalues with one dominant eigenmode to complex-valued eigenvalues with two dominant eigenmodes is steep, as shown in Fig. 1, provided that $m \geq 2$ and m is not too large. The case $m=1$ (not shown in Fig. 1) is somewhat singular and such a transition is not sharp and occurs at high values of Δ_f . At such high values of Δ_f , the amplitude modulation acts as a perturbation, the pulse shaping being provided by the frequency modulation as in a FM mode-locked laser; in this case the pulse splitting corresponds merely to the existence of the well-known up- and down-chirped FM pulses (see, e.g., Ref. [15]). Likewise, at high values of the harmonic order m , such that the period T_m/m of the phase modulation becomes smaller than the pulse width of the AM mode-locked laser without the phase perturbation, the transition from real valued to complex-conjugate eigenvalues is more involved and shows successive eigenvalue crossings; in addition, the dominant eigenmodes deviate from a Gaussian shape. This case will be not considered here.
- [26] S. Longhi, *Opt. Commun.* **188**, 239 (2001).
- [27] Note that since $\mathcal{L}^\dagger(t) = \gamma\partial/\partial t + \mathcal{D}_g\partial^2/\partial t^2 + \Delta[\cos(2\pi t) - 1] + i\Delta_f \sin(2\pi mt) \neq \mathcal{L}(t)$, the mode-locking operator \mathcal{L} is not self-adjoint, so that in general $\Phi_n^\dagger(t) \neq \Phi_n(t)$. $\mathcal{L}(t)$ is self-adjoint solely in absence of the phase modulation ($\Delta_f=0$) and for zero detuning ($\gamma=0$). For $\gamma=0$, one can easily show that apart for a normalization factor, $\Phi_n^\dagger = \Phi_n^*$.